

Article

Oxidative Conversion of Chars Generated from the Fixed-Bed Pyrolysis of Wood Torrefied at Different Temperatures and Holding Times

Carmen Branca ^{1,*}  and Colomba Di Blasi ²

¹ Istituto di Scienze e Tecnologie per l'Energia e la Mobilità Sostenibili (STEMS), C.N.R., P.le V. Tecchio, 80125 Napoli, Italy

² Dipartimento di Ingegneria Chimica, dei Materiali e della Produzione Industriale, Università degli Studi di Napoli "Federico II", P.le V. Tecchio, 80125 Napoli, Italy; diblasi@unina.it

* Correspondence: carmen.branca@stems.cnr.it; Tel.: +39-081-7682232

Abstract: Fixed-bed pyrolysis of torrefied spruce wood, for a heating temperature of 800 K, results in char yields between about 27–57 wt% (versus 23 wt% for untreated wood), depending on both pre-treatment temperatures (533–583 K) and holding times (8–25 min). In this study char oxidation behavior and kinetics are investigated by means of thermogravimetric analysis. The differential thermogravimetric curves always showed a low-temperature zone of slow rates (oxidative devolatilization), followed by a high-rate zone with a well-defined peak (oxidation). As the torrefaction severity increases, the temperature range of the oxidative devolatilization enlarges. Moreover, the oxidation rates become slower (both burning and burnout temperatures tend to increase). As already found for untreated wood chars, the two stages are well described by a linear and a power-law rate reaction, respectively. Volatiles released from the devolatilizations are approximately around 20 wt%, but torrefaction causes lower activation energies (66–92 kJ/mol versus 117 kJ/mol). The oxidation activation energies also decrease (170–168 kJ/mol versus 193 kJ/mol), accompanied by small variations in the reaction order.

Keywords: pyrolysis; torrefaction; char oxidation; thermogravimetry; kinetics



Citation: Branca, C.; Di Blasi, C. Oxidative Conversion of Chars Generated from the Fixed-Bed Pyrolysis of Wood Torrefied at Different Temperatures and Holding Times. *Processes* **2023**, *11*, 997. <https://doi.org/10.3390/pr11040997>

Academic Editor: Song Hu

Received: 6 March 2023

Revised: 20 March 2023

Accepted: 21 March 2023

Published: 24 March 2023



Copyright: © 2023 by the authors. Licensee MDPI, Basel, Switzerland. This article is an open access article distributed under the terms and conditions of the Creative Commons Attribution (CC BY) license (<https://creativecommons.org/licenses/by/4.0/>).

1. Introduction

Torrefaction, a mild pyrolysis, is a pre-treatment for improving chemico-physical properties of biomass which, in this way, tend to approach those of coal [1]. Dry or wet torrefaction technologies have been proposed, and efforts are still under way (for instance, see Refs. [2,3]) to improve the process efficiency. On the other hand, the pyrolysis of torrefied biomass gives rise to modified yields and properties of the three lumped classes of products, that is, gas, char and bio-oil [4]. When fuel applications are considered for the char product [5], a key issue is the oxidation reactivity, which is affected by numerous factors [6]. In fact, experimental evidence exists, supported by several studies [7–16], that chars from torrefied biomass are less reactive, though there is no consensus about the magnitude of the reduction and the specific causes for such variations, also owing to differences in the analysis conditions and origin materials.

Fisher et al. (2012) [7] examined the effects of torrefaction (willow wood) for both fast- (1173 K with 2 s holding time) and slow- (33 K/min up to 1073–1273 K, 30 min or 1 h holding time) heating rate chars. The reduction in the reactivity was higher for the former, which was attributed to enhanced exposure to high temperatures. Reactivity also increased from coal to torrefied willow char and to raw willow char [8], with torrefaction also affecting nitrogen partitioning between the solid and gas phase. Palm kernel shells chars, produced under high temperatures and heating rates, subjected to combustion, again exhibited reduced reactivity in the presence of the torrefaction pre-treatment [9], especially

for the initial stage. The carbon conversion rate was slowed for both combustion and gasification by the torrefaction pre-treatment for chars from forest residues pyrolyzed in a drop tube reactor (1473 K at a heating rate greater than 104 K/s) [10]. Further investigation confirmed that chars produced from torrefied materials were less reactive than those from raw materials, with quantitative differences depending on the wood variety [11]. Combustion experiments at the particle/pellet scale [12–14] for torrefied materials also reported important changes for the various conversion stages. In fact, the unmodified reactivity of thick torrefied wood particles was associated with longer conversion times [14]. Ignition, devolatilization and char combustion required longer times, as a consequence of a wet torrefaction pre-treatment (Schima wood) [12]. This also caused modifications in the content of alkali metals, with a remarkable decrease in the char combustion rate. For mild torrefaction-treated pellets (rice straw, pine wood, cornstalk), the following features were observed [13]: shorter ignition delay, higher volatile combustion flame height and peak temperature, longer volatile and char combustion duration, and lower peak char combustion temperature.

Thermogravimetric measurements of torrefied biomass under oxidative conditions revealed that both the devolatilization and the oxidation stage were affected by the pre-treatment [15,16], resulting from a modified chemical composition of the torrefied versus the untreated materials. These effects are described by modified parameters for the multi-step schemes for oxidative pyrolysis. The influences of torrefaction on the global oxidation kinetics were discussed in [9,11], only for chars produced under fast heating. For both cases, modifications in the kinetic parameters were reported. However, it is well known that a single-step reaction for the biomass char oxidation leads to highly underestimated activation energies [6], so that two-step reaction schemes are required for accurate process descriptions. Indeed, two stages are always shown by the oxidation curves of chars generated from untreated biomass [6,17–24]. However, how torrefaction modifies the kinetic parameters of the two-step scheme for the char oxidation is not known. Moreover, the influences of torrefaction for char produced for the conditions of interest in fixed-bed combustion and gasification have not yet been studied. In this study, the oxidative conversion of chars produced from torrefied wood, after pyrolysis under the moderate heating rates of a packed-bed reactor, was investigated by means of thermogravimetric and kinetic analyses. The changes induced in the thermogravimetric and kinetic parameters by the severity of the torrefaction pre-treatment are discussed, starting from results obtained for untreated wood using two-step reaction schemes.

2. Materials and Methods

In this section, the wood torrefaction pretreatments are first briefly outlined. Then, the conditions of the pyrolysis system where the char samples were produced and the thermogravimetric measurements are described. Finally, the kinetic model and the numerical methods are presented.

2.1. Char Formation and Thermogravimetric Conditions

Untreated and torrefied spruce wood (*Picea abies*) was used for the fixed-bed pyrolysis. The torrefaction conditions were the same as those already reported elsewhere [15], and achieved using an electrically heated rotating drum. Both temperatures (533–583 K) and holding times (8–25 min) were varied, as indicated in Table 1. The torrefaction conditions and the yields of torrefied product, expressed as percent on a dry mass basis, are reported here. It is useful to recall that torrefaction is generally established at temperatures around 473–573 K, and solid retention times from several minutes to about 1 h, leading to solid product yields of around 70 wt% [15]. According to this range of conditions, only samples b–d are truly representative of torrefaction conditions of practical interest (torrefied product yields between 89–76.5 wt%). In fact, although the treatment temperature of sample d was slightly higher than the upper limit, the torrefied product yield is still above 70 wt%. Instead, the long retention time and high temperature of sample e resulted in a very severe

treatment, with a torrefied product yield of around 46 wt%, which is essentially carbonized wood. Untreated wood (sample a) is considered for comparison.

Table 1. Yields (wt%) of torrefied product, Y_{tor} , and char from fixed-bed pyrolysis at 800 K, Y_{char} , for spruce wood pre-treated at temperature, T_{tor} , for holding time, t_{tor} , [15,25].

Char Sample	T_{tor} [K], t_{tor} [min]	Y_{tor} [wt%]	Y_{char} [wt%]
a	untreated wood	100	22.7
b	533 K, 25 min	89.2	27.7
c	558 K, 16.5 min	80.3	30.7
d	583 K, 8 min	76.5	32.3
e	583 K, 25 min	45.9	57.3

Table 1 also reports the char yields obtained from packed-bed pyrolysis carried out at 800 K [25]. The pyrolysis reactor set-up has already been described in detail in previous research [26–29] (schematic reported in [27]). In summary, it is a cylindrical steel reactor where nitrogen, top-fed flows through a jacket, is heated by an electrical furnace and distributed at the bottom by a perforated steel plate. This also supports the packed bed whose thermal conditions are monitored by seven thermocouples along the reactor axis. The packed bed is positioned along the lower reactor zone where isothermal conditions are achieved, as determined by the furnace set point.

The pyrolysis experiments were conducted when a steady temperature of 800 K was reached. After nitrogen flushing, the sample (about 150 g) was suddenly (about 40 s) dropped inside the pre-heated reactor. The char yields vary between 28–57 wt% (versus 23 wt% of untreated wood). Given approximately constant gas yield, the increase in the char yields is compensated by a decrease in the liquid yields. These, however, are enriched by anhydro-sugars, guaiacols possessing a carbonyl group, and phenols. It was also found that the yields of fixed-bed pyrolysis char, when referred to the initial mass of untreated material before torrefaction, are barely higher than that of the untreated wood (25 versus 23 wt%). The increase is larger for the charred sample (26 wt%). Therefore, it can be stated that the prolonged exposure to moderate temperatures favors cross-linking reactions, justifying not only higher char yields but also modified microstructures. The sample thermal dynamics were weakly affected by the pre-treatment, though convective cooling was reduced (reduction in the volatile product yields). Moreover, the global pyrolysis exothermicity, important for different configurations and materials [30,31], appeared to be small.

It is useful to note that as the torrefaction severity increases, the yields of torrefied product, Y_{tor} , become successively lower (from 100 to 46 wt%, Table 1). Instead, the char yields, Y_{char} , from the fixed-bed pyrolysis become progressively higher, with values increasing from about 23 to 57 wt%, again for the limit conditions of Table 1. Hence, the variable Y_{char} is used in the following to define the severity level of torrefaction (the higher the char yield is, the more severe the torrefaction of wood).

For the thermogravimetric analysis, the chars are milled to obtain particle sizes below 80 μm , and pre-dried for 10 h at 373 K. The measurements use a specifically designed system that allows for an effective control of the sample temperature and negligible mass transfer limitations for both the oxidant and the oxidation products, as already described in previous research [17,19,20,23,32–36]. A sample mass of 4 mg, corresponding to a layer thickness around 100 μm (the characteristic process size), is subjected to a heating rate of 5 K/min up to 840 K in air. Measurements, made in triplicate, show good repeatability (maximum deviations in the weight loss curves were always in the range of 0.1–0.3%). These curves are subjected to kinetic analysis.

2.2. Kinetic Modelling

The kinetic evaluation of the curves obtained for the various samples was carried out using a mechanism consisting of two parallel reactions for char devolatilization and

oxidation, and starting from the results already obtained for the char from untreated spruce wood [24]:



where C_1 and C_2 are the two char fractions undergoing oxidative devolatilization (d) and oxidation (b), which produce the lumped volatile products, V_1 and V_2 , respectively.

The reaction rates present an Arrhenius dependence on temperature (A_d and A_b are the pre-exponential factors, and E_d and E_b are the activation energies) and a linear (devolatilization) or power-law (n_b , oxidation) dependence on the solid mass fraction. The stoichiometric coefficient (the volatile mass fraction generated by the devolatilization reaction), v_d , is also introduced (the fraction concerning oxidation, v_b , can be obtained by difference). The sample temperature, T , is a known function of time, so that the mathematical model consists of two ordinary equations for the mass fractions, Y_i , of volatiles generated from each pseudo-component i :

$$-\frac{dY_1}{dt} = A_d \exp(-E_d/RT) Y_1, Y_1(0) = v_d \quad (3)$$

$$-\frac{dY_2}{dt} = A_b \exp(-E_b/RT) Y_2^{n_b}, Y_2(0) = v_b \quad (4)$$

The kinetic parameters were numerically estimated through the numerical solution (routine `ode15s` of the software MATLAB (MathWorks, Natick, MA, USA), release R2017b) of the mass conservation Equations (3) and (4), and the minimization (routine `fminsearch`) of the objective function based on the least-squares method essentially using the time derivatives of the mass fractions according to the procedure already described elsewhere [17,21,23,32,36]. The parameters to be estimated for each sample are the activation energies (E_d , E_b), the pre-exponential factors (A_d , A_b), the reaction order n_b , and the stoichiometric coefficient v_d . The deviations between measurements and model predictions, dev_{TG} and dev_{DTG} , for the integral and differential data, respectively, are evaluated using Equations (5) and (6), also defined in accordance with previous analyses [32]:

$$\%dev = \frac{\sqrt{S/N}}{(\Phi_i)_{exp,peak}} \times 100 \quad (5)$$

$$S = \sum_{i=1,N} ((\Phi_i)_{exp} - (\Phi_i)_{sim})^2 \quad (6)$$

where i represents the experimental (*exp*) or the simulated (*sim*) variable (Φ is the solid mass fraction, Y , or the devolatilization rate, $-dY/dt$) at time t (N is the number of experimental points, and the subscript “*peak*” indicates the maximum value).

3. Results

The main features of the thermogravimetric curves are first examined with the aid of parameters introduced for lignocellulosic char oxidation, followed by kinetic evaluation. The modifications induced by the torrefaction pre-treatment on the thermogravimetric and kinetic parameters are discussed.

3.1. Thermogravimetric Curves

The influences of the torrefaction on the reactivity of the fixed-bed pyrolysis chars can be observed by means of the weight loss curves reported in Figure 1 for the various samples. At a first glance, it appears that the chief features of the conversion process are not modified by the pre-treatment. The curves show an initial zone of very slow weight loss (temperatures approximately below 650–660 K), followed by a very rapid conversion

testified by the attainment of a high and well-defined peak rate. These two zones are associated with char devolatilization and oxidation [6]. As for the first zone, the chars from torrefied wood initially exhibit barely higher (temperatures below 600 K) and then lower rates than untreated wood. Moreover, the peak of the oxidation rate slightly decreases, as a consequence of the torrefaction, and moved at higher temperatures. Most likely as a consequence of the moderate heating rates reached during pyrolysis, the overall effects of the torrefaction pre-treatment on the char reactivity are small, but differences in the shape of the rate curve may introduce non-negligible changes in the chemical kinetics.

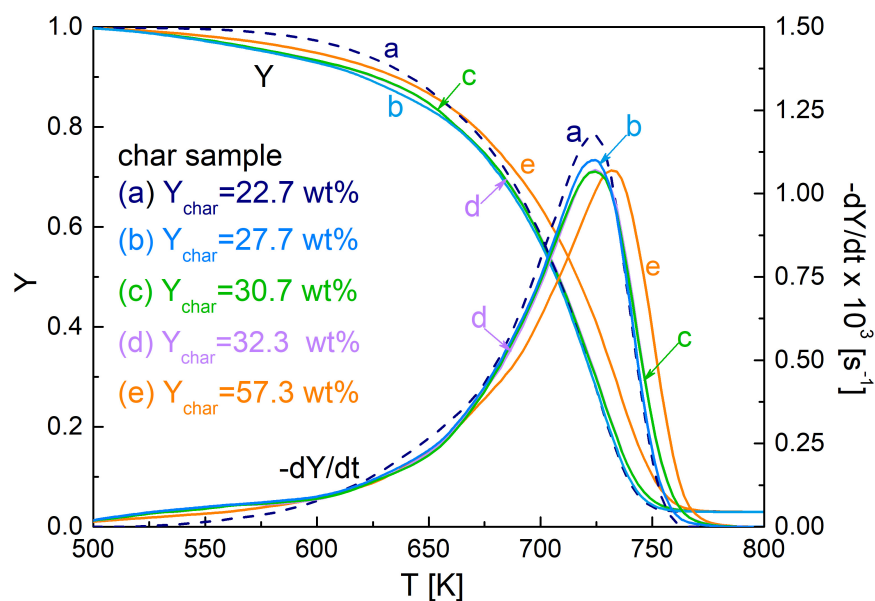


Figure 1. Weight loss curves (Y) and devolatilization rate curves ($-dY/dt$) as functions of temperature for the oxidation of fixed-bed chars produced at 800 K, from untreated and torrefied spruce wood (torrefaction conditions in Table 1) measured for a heating rate of 5 K/min.

To quantify the torrefaction effects on char oxidation, it was useful to introduce some parameters [24], as indicated in Figure 2. Together with the peak rate, dY_b , the corresponding temperature, T_b , and mass fraction, Y_b , were considered. Moreover, two temperatures are introduced, T_{ign} and $T_{burnout}$, for identifying the temperature range where oxidation took place. The temperature T_{ign} is defined by extrapolating the slope of the rate curve in correspondence of the local maximum in $-d^2Y/dt^2$ up to the zero level of the Y axis. The temperature $T_{burnout}$ of the final tailing zone of the curve is obtained by extrapolating the rate corresponding to the minimum in $-d^2Y/dt^2$ up to the zero level of the Y axis. Then, the temperature range $\Delta T_{ox} = T_{burnout} - T_{ign}$ identifies the zone where oxidation occurs. The temperature T_{ign} roughly demarcates the conclusion of the devolatilization stage. The corresponding mass fraction, Y_{ign} , provides an indication about the amount of char being converted during the oxidation stage. The initial temperature for devolatilization, T_i , corresponding to a mass fraction of 0.98, was also introduced, with the temperature range for devolatilization, defined as $\Delta T_{dev} = T_{ign} - T_i$.

The above defined parameters are reported as functions of the pyrolysis char yield (and thus, the torrefaction degree) in Figure 3A,B. The demarcation temperature between oxidative devolatilization and oxidation, T_{ign} , slightly increases with the torrefaction degree (variation range of 660–666 K), also associated with mass fractions, Y_{ign} , varying from about 0.84 to 0.8. Hence, the mass fraction, available for the oxidation stage slightly decreases (the ash content also increases with the severity of the thermal treatment [15,26]), with values for the char samples increasing from about 1 to 1.8 wt% for the two extreme conditions. Moreover, the oxidation is also characterized by increasing values of the peak rate temperature, T_b , (723–732 K) and the burnout temperature, $T_{burnout}$, (752–763 K), so that the temperature range of interest also enlarges (ΔT_{ox} from 92 to about 97 K). Based

on these findings, it can be speculated that, although the peak oxidation rate only weakly changes, the average oxidation rate decreases. Oxidative devolatilization occurs over a wide temperature range for the chars from torrefied wood, owing to, on one side, the enhanced rates at low temperatures (this effect is smaller for the carbonized wood sample) and, on the other, to the beginning of the actual oxidation at higher temperatures. This is shown by the temperature range, ΔT_{dev} , also reported versus the char yield.

The reduction in the oxidation rate (and the reactivity) of chars from torrefied wood, observed in this study, agrees with the results previously reported by other authors [7–16]. As already observed, the chars originating from torrefied wood undergo a longer exposure to temperatures apt to initiate (torrefaction) and complete (pyrolysis) the conversion process. The release of volatile products is also associated with the formation of char, whose properties (in particular, aromaticity) depend on the thermal conditions (temperature and holding time) of the treatment, which then affect the related reactivity [6]. The torrefaction process also modify the relative contents of the three main macro-components [37], as well as their structure and the mutual interaction during pyrolysis. In fact, torrefaction concerns not only the decomposition of hemicellulose, to an extent that depends on the thermal conditions, but cellulose and lignin are also involved. Thus, the different composition and properties of the substrate are other factors that may play a role in the char properties. The thermal pre-treatment also induces changes in the association of inorganic components [38], specifically the distribution of calcium, magnesium and manganese, with modification also in the water solubility of potassium compounds, probably as a consequence of the destruction of carboxylic acid groups. Given the importance of the catalytic action exerted by indigenous metals, it is expected that not only pyrolytic conversion, but also char oxidation, may be consequently modified.

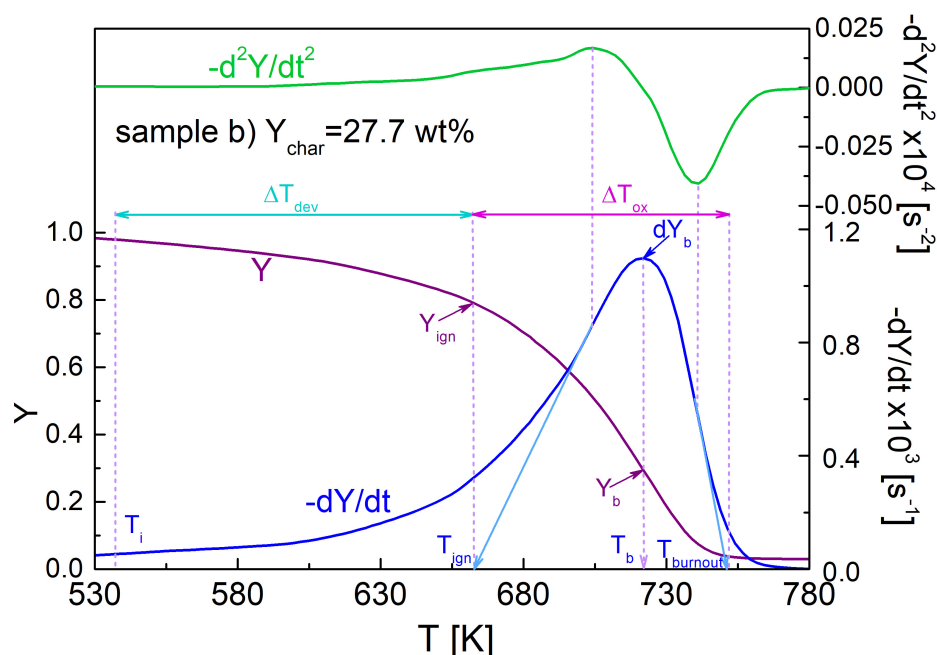


Figure 2. Mass fraction, Y , and first, $-dY/dt$, and second, $-d^2Y/dt^2$, time derivatives of the mass fraction, showing the thermogravimetric parameters: peak rate, dY_b , and corresponding temperature, T_b , and mass fraction, Y_b . The temperatures for the beginning and completion of char oxidation, T_{ign} and $T_{burnout}$, respectively, and corresponding temperature interval, $\Delta T_{ox} = T_{burnout} - T_{ign}$, the char mass fraction, Y_{ign} , in correspondence of T_{ign} , the initial temperature for devolatilization, T_i , and the temperature range for devolatilization, $\Delta T_{dev} = T_{ign} - T_i$, are also shown.

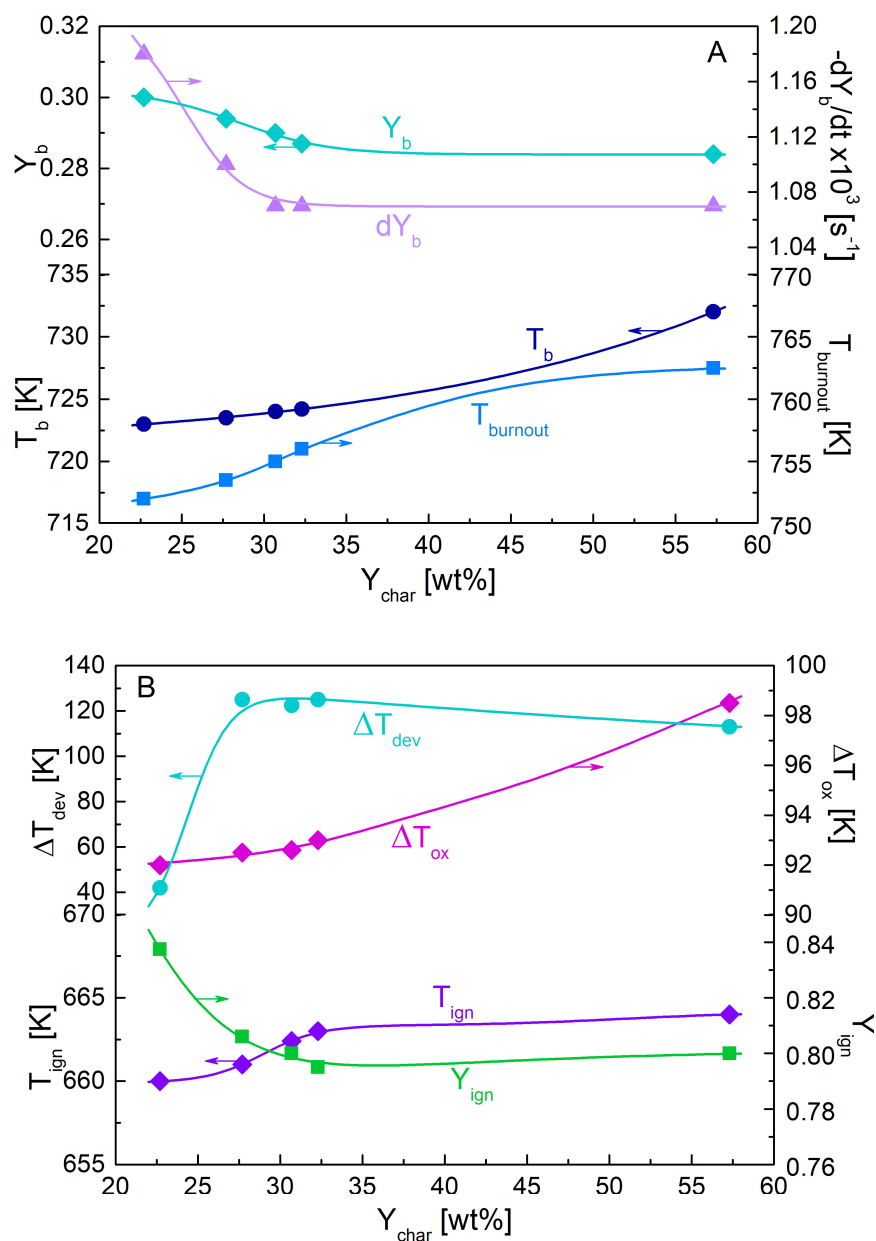


Figure 3. Thermogravimetric parameters dY_b , T_b , Y_b , $T_{burnout}$ (A), and T_{ign} , Y_{ign} , ΔT_{ox} and ΔT_{dev} (B), versus the torrefaction degree expressed in terms of pyrolysis char yield, Y_{char} .

3.2. Kinetic Parameters

The kinetic evaluation of the thermogravimetric curves for samples a-e, starting from the values already available for the oxidation of chars from untreated spruce wood [23], lead to the results summarized in Table 2. In order to understand the changes introduced by the torrefaction on the oxidation kinetics (second reaction step), the triangular plots of Figure 4 can be examined, where the peak rates are reported on a temperature scale using the three characteristic values, T_{ign} , T_b and $T_{burnout}$, all increasing with the severity of the pre-treatment. These clearly show how the slopes of the differential thermogravimetric curves, which determine the activation energy and reaction order, are modified. The first part of the plot (left-hand side) shows decreasing slopes from the untreated to carbonized wood char, whereas for the intermediate (torrefaction) conditions, it is practically constant. This trend shows decreasing activation energies as the torrefaction level increases. On the other hand, for the right-hand side, the slope decreases, indicating that, in principle, the

reaction order increases as the torrefaction becomes more severe. In this case, however, a compensation effect with the activation energy should be considered.

Table 2. Estimated kinetic parameters (activation energy, E , pre-exponential factor, A , reaction order, n , and stoichiometric coefficient, ν , for the devolatilization (d) and oxidation (b) reactions, and deviations between predicted and measured integral and differential curves, dev_{TG} and dev_{DTG} , respectively, for the pyrolysis chars (torrefaction conditions listed in Table 1).

Parameter	Char Sample, Y_{char} [wt%]				
	(a) 22.7	(b) 27.7	(c) 30.7	(d) 32.3	(e) 57.3
E_d [kJ/mol]	117.0	66.0	66.8	66.6	91.7
A_d [s^{-1}]	5.9×10^6	4.70×10^2	5.09×10^2	4.97×10^2	4.85×10^4
ν_d	0.17	0.18	0.18	0.19	0.19
E_b [kJ/mol]	192.8	170.2	169.8	169.8	167.7
A_b [s^{-1}]	3.0×10^{11}	6.05×10^9	9.85×10^9	5.47×10^9	2.82×10^9
n_b	0.89	0.83	0.866	0.87	0.81
dev_{TG} [%]	1.10	1.48	1.38	1.36	1.46
dev_{DTG} [%]	0.69	0.68	0.68	1.21	0.92

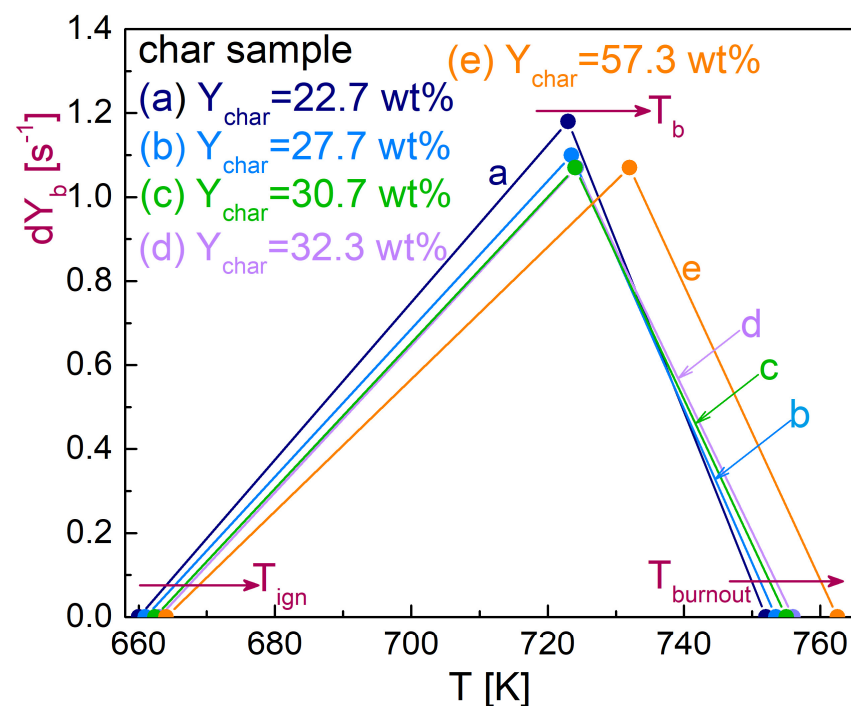


Figure 4. Peak rate versus temperature, using the three characteristic values, T_{ign} , T_b and T_{burnout} , for the various char samples (torrefaction conditions as shown in Table 1).

In accordance with the above analysis, the estimated activation energies of the oxidation reaction decreases as the torrefaction level increases, as reported in Table 2 and Figure 5, though the variations are not exceedingly high (values between 170–168 kJ/mol for the chars from torrefied wood with respect to 193 kJ/mol in the absence of pre-treatment). The dependence of the ratio between activation energy and reaction order (this was only weakly variable) (Figure 5) presents a minimum for sample d just before carbonization is achieved (sample e) (values in the range of 195–217 kJ/mol). This finding agrees with the results provided by kinetic analysis methods based on the peak rate properties [39], yielding values in the range of 183–206 kJ/mol. It is worth observing that the oxidation activation energies preserve the high values reported for lignocellulosic chars, when devolatilization is described by a separate step [6].

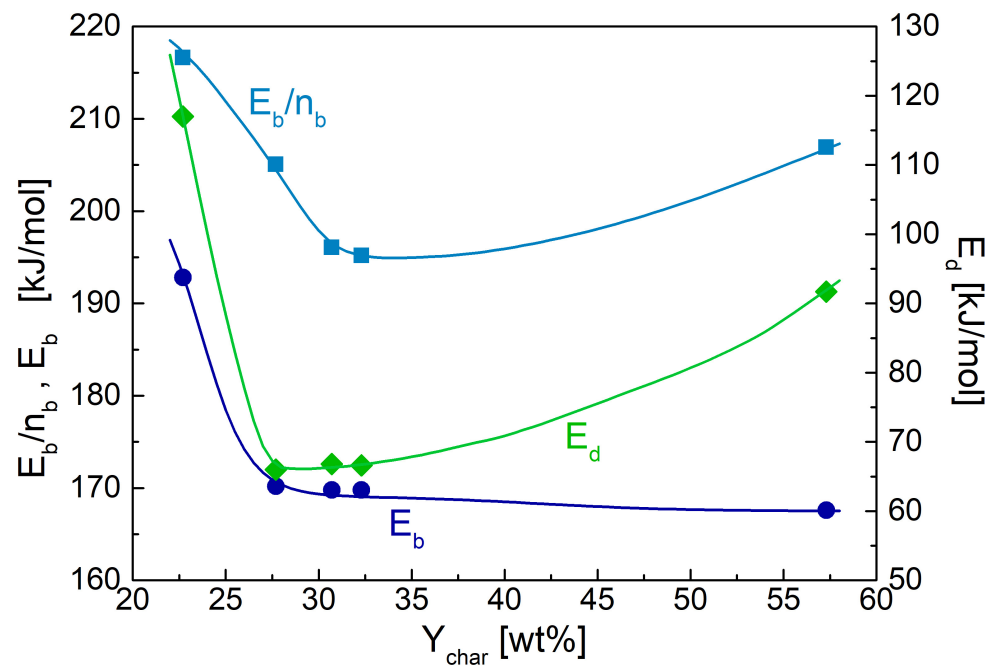


Figure 5. Activation energies of the devolatilization reaction, E_d , and the oxidation reaction, E_b , and ratio E_b/n_b (n_b reaction order) versus the torrefaction degree expressed in terms of pyrolysis char yield, Y_{char} .

The activation energies of the devolatilization stage show a trend on dependence of the torrefaction degree that is qualitatively similar with that of the above ratio, with values always lower for the pre-treated samples (62–92 kJ/mol versus 117 kJ/mol) (Table 2, Figure 5). Decreasing values of the activation energies are associated with the enlargement of the temperature range where the process takes place for the chars from torrefied wood. However, as already commented above, the enlargement is lower for the sample related to carbonized wood, justifying the final increase in the activation energy.

A quantitative comparison with previous kinetic analyses is not possible, owing to the application of a single-step reaction and chars produced under fast heating rates [9,11]. However, it is interesting to note that, for both cases, the reduced reactivity leads to modifications in the activation energy and reaction order. For instance, in [9] the activation energy varies from 47.5 to 60 kJ/mol, and the reaction order from 0.29 to 0.8.

The agreement between the predictions of the model and the measurements is very good, as indicated by the small deviations (Table 2), and by the comparison between measured and predicted curves reported in Figure 6A–D for samples a, b, d, e. The component dynamics, also reported in Figure 6A–D, always show significant overlap, confirming the need to apply model-fitting methods to obtain accurate process kinetics.

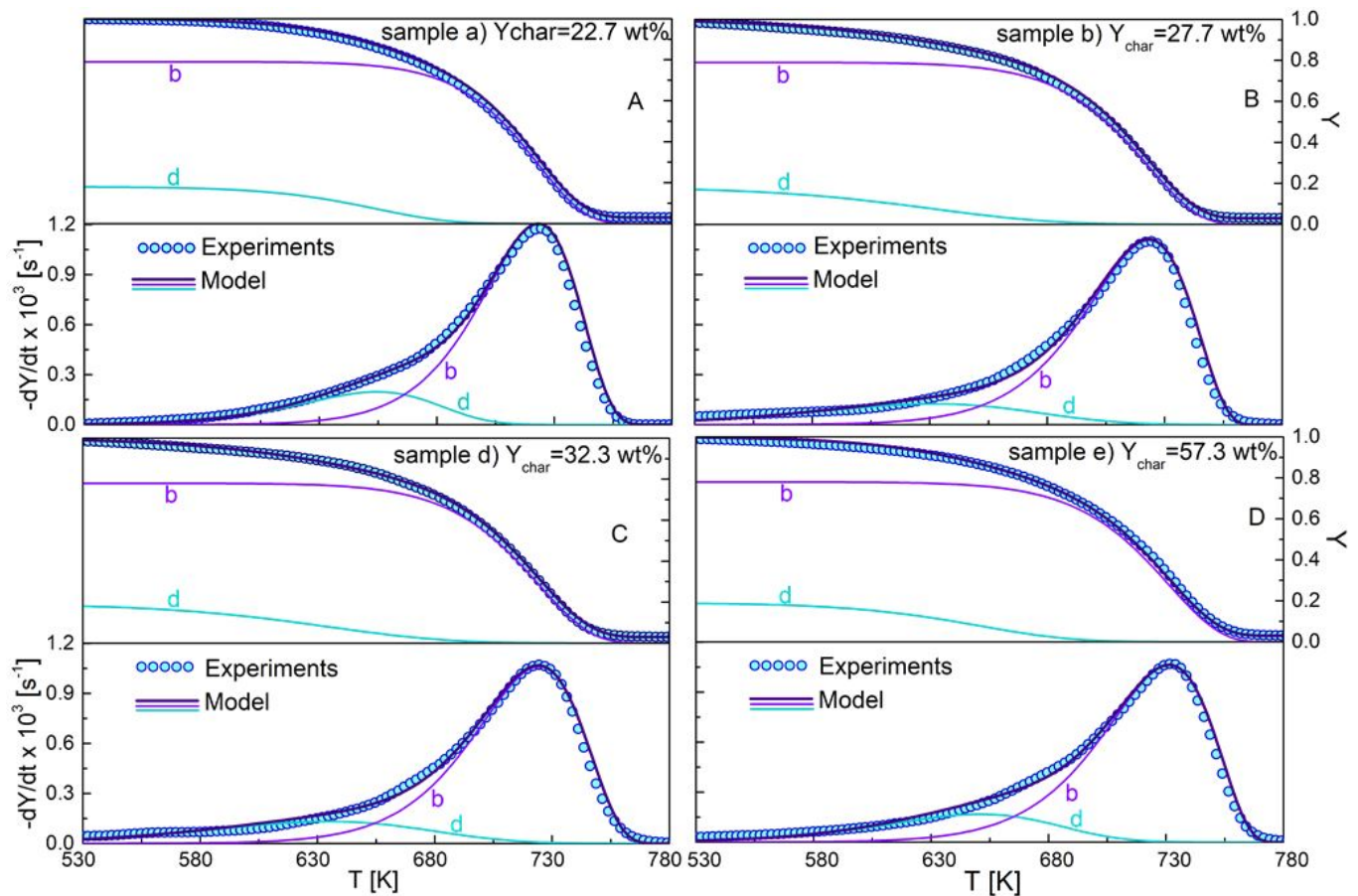


Figure 6. Weight loss curves (Y) and devolatilization rate curves ($-dY/dt$) for the pyrolysis chars samples a (A), b (B), d (C) and e (D) (torrefaction conditions in Table 1) versus temperature, as measured (symbols) and predicted (solid lines) (including the prediction for the devolatilization (d) and oxidation (b) reactions).

4. Conclusions

The oxidation behavior of chars, produced from the fixed-bed pyrolysis of torrefied wood, was investigated by means of thermogravimetric analysis. Although the usual zones of char oxidative devolatilization and oxidation are observed, the thermal pre-treatment causes important quantitative modifications. In general, torrefaction increases the importance of the devolatilization, which occurs over wider temperature ranges. Oxidation is displaced at higher temperatures and, on the average, occurs at slower rates.

The thermogravimetric curves of char oxidation are well described by a two-step reaction scheme whose parameters are significantly affected by the torrefaction pre-treatment. For both cases, the estimated activation energies are lower than those obtained for the chars from untreated wood, with values in the range of 66–92 kJ/mol (versus 117 kJ/mol) and 170–168 kJ/mol (versus 193 kJ/mol) for the devolatilization and oxidation, respectively. The severity of the torrefaction is important, especially for the most extreme conditions corresponding to carbonization, and should be considered when the conversion of torrefied material is of interest.

It appears that, globally, the effects of torrefaction on the oxidation of wood chars produced under moderate thermal conditions are not exceedingly high. From the qualitative point of view, they are similar with those observed for fast- and high-temperature pyrolysis. The chemical kinetics are remarkably modified. Further investigation is required about the chemico-physical factors leading to modified char reactivity.

Author Contributions: Conceptualization, C.B. and C.D.B.; methodology, C.B. and C.D.B.; investigation, C.B. and C.D.B.; data curation, C.B. and C.D.B.; writing, review and editing, C.B. and C.D.B. All authors have read and agreed to the published version of the manuscript.

Funding: This research received no external funding.

Institutional Review Board Statement: Not applicable.

Informed Consent Statement: Not applicable.

Data Availability Statement: The data supporting the findings of this study are available within the article.

Conflicts of Interest: The authors declare no conflict of interest.

References

1. Teh, J.S.; Teoh, Y.H.; How, H.G.; Sher, F. Thermal analysis technologies for biomass feedstocks: A state-of-the-art review. *Processes* **2021**, *9*, 1610. [[CrossRef](#)]
2. Silveira, E.A.; Oliveira Galvão, L.G.; Alves de Macedo, L.; Sá, I.A.; Chaves, B.S.; Girão de Moraes, M.V.; Rousset, P.; Caldeira-Pires, A. Thermo-acoustic catalytic effect on oxidizing woody torrefaction. *Processes* **2020**, *8*, 1361. [[CrossRef](#)]
3. Mutlu, Ö.; Roy, P.; Zeng, T. Downstream torrefaction of wood pellets in a rotary kiln reactor—Impact on solid biofuel properties and torr-gas quality. *Processes* **2022**, *10*, 1912. [[CrossRef](#)]
4. Kumar, R.; Strezov, V.; Weldekidan, H.; He, J.; Singh, S.; Kan, T.; Dastjerdi, B. Lignocellulose biomass pyrolysis for bio-oil production: A review of biomass pre-treatment methods for production of drop-in fuels. *Renew. Sustain. Energy Rev.* **2020**, *123*, 109763. [[CrossRef](#)]
5. Sen, A.U.; Pereira, H. State-of-the-art char production with a focus on bark feedstocks: Processes, design, and applications. *Processes* **2021**, *9*, 87. [[CrossRef](#)]
6. Di Blasi, C. Combustion and gasification rates of lignocellulosic chars. *Prog. Energy Combust. Sci.* **2009**, *35*, 121. [[CrossRef](#)]
7. Fisher, E.M.; Dupont, C.; Darvell, L.I.; Commandré, J.-M.; Saddawi, A.; Jones, J.M.; Grateau, M.; Nocquet, T.; Salvador, S. Combustion and gasification characteristics of chars from raw and torrefied biomass. *Bioresour. Technol.* **2012**, *119*, 157. [[CrossRef](#)] [[PubMed](#)]
8. Jones, J.M.; Bridgeman, T.G.; Darvell, L.I.; Gudka, B.; Saddawi, A.; Williams, A. Combustion properties of torrefied willow compared with bituminous coals. *Fuel Proc. Technol.* **2012**, *101*, 1. [[CrossRef](#)]
9. Li, J.; Bonvicini, G.; Biagini, E.; Yang, W.; Tognotti, L. Characterization of high-temperature rapid char oxidation of raw and torrefied biomass fuels. *Fuel* **2015**, *143*, 492. [[CrossRef](#)]
10. Li, T.; Geier, M.; Wang, L.; Ku, X.; Matas Güell, B.; Løvas, T.; Shaddix, C.R. Effect of torrefaction on physical properties and conversion behavior of high heating rate char of forest residue. *Energy Fuels* **2015**, *29*, 177. [[CrossRef](#)]
11. McNamee, P.; Darvell, L.I.; Jones, J.M.; Williams, A. The combustion characteristics of high-heating-rate chars from untreated and torrefied biomass fuels. *Biomass Bioenergy* **2015**, *82*, 63. [[CrossRef](#)]
12. Lu, Z.; Li, X.; Jian, J.; Yao, S. Flame combustion of single wet-torrefied wood particle: Effects of pretreatment temperature and residence time. *Fuel* **2019**, *250*, 160. [[CrossRef](#)]
13. Li, K.; Yan, W.; Huang, X.; Yu, L.; Zhou, H. In-situ measurement of combustion characteristics and potassium release concentration during torrefied biomass burning based on spontaneous emission spectroscopy. *Fuel* **2022**, *328*, 125249. [[CrossRef](#)]
14. Lu, Z.; Jian, J.; Arendt Jensen, P.; Wu, H.; Glarborg, P. Impact of KCl impregnation on single particle combustion of wood and torrefied wood. *Fuel* **2017**, *206*, 684. [[CrossRef](#)]
15. Broström, M.; Nordin, A.; Pommer, L.; Branca, C.; Di Blasi, C. Influence of torrefaction on the devolatilization and oxidation kinetics of wood. *J. Anal. Appl. Pyrolysis* **2012**, *96*, 100. [[CrossRef](#)]
16. Tapasvi, D.; Khalil, R.; Várhegyi, G.; Skreiberg, Ø.; Tran, K.; Grønli, M. Kinetic behavior of torrefied biomass in an oxidative environment. *Energy Fuels* **2013**, *27*, 1050. [[CrossRef](#)]
17. Branca, C.; Di Blasi, C. Devolatilization and combustion kinetics of wood chars. *Energy Fuels* **2003**, *17*, 1609. [[CrossRef](#)]
18. Várhegyi, G.; Meszaros, E.; Antal, M.J.; Bourke, J.; Jakab, E. Combustion kinetics of corncob charcoal and partially demineralized corncob charcoal in the kinetic regime. *Ind. Eng. Chem. Res.* **2006**, *45*, 4962. [[CrossRef](#)]
19. Branca, C.; Di Blasi, C. Combustion kinetics of secondary biomass chars in the kinetic regime. *Energy Fuels* **2010**, *24*, 5741. [[CrossRef](#)]
20. Branca, C.; Di Blasi, C. Thermogravimetric analysis of the combustion of dry distiller's grains with solubles (DDGS) and pyrolysis char under kinetic control. *Fuel Process. Technol.* **2015**, *129*, 67. [[CrossRef](#)]
21. Branca, C.; Di Blasi, C. Self-heating effects in the thermogravimetric analysis of wood char oxidation. *Fuel* **2020**, *276*, 118012. [[CrossRef](#)]
22. Branca, C.; Di Blasi, C. Burning dynamics of straw chars under the conditions of thermal analysis. *Energy Fuels* **2021**, *35*, 12187. [[CrossRef](#)]

23. Branca, C.; Di Blasi, C. Effects of heat/mass transfer limitations and process exothermicity on the kinetic parameters of the devolatilization and oxidation reactions of wood chars. *Thermochim. Acta* **2022**, *716*, 179321. [[CrossRef](#)]
24. Branca, C.; Di Blasi, C. Enhancement and inhibition of the oxidation rates of pyrolytic chars from wood loaded with potassium compounds. *Fuel* **2023**, *331*, 125886. [[CrossRef](#)]
25. Branca, C.; Di Blasi, C.; Galgano, A.; Brostrom, M. Effects of the torrefaction conditions on the fixed-bed pyrolysis of Norway spruce. *Energy Fuels* **2014**, *28*, 5882. [[CrossRef](#)]
26. Di Blasi, C.; Branca, C.; Galgano, A. Effects of diammonium phosphate on the yields and composition of products from fir wood pyrolysis. *Ind. Eng. Chem. Res.* **2007**, *46*, 430. [[CrossRef](#)]
27. Di Blasi, C.; Branca, C.; Galgano, A. Biomass screening for furfural production via thermal decomposition. *Ind. Eng. Chem. Res.* **2010**, *49*, 2658. [[CrossRef](#)]
28. Branca, C.; Di Blasi, C.; Galgano, A. Pyrolysis of corncobs catalyzed by zinc chloride for furfural production. *Ind. Eng. Chem. Res.* **2010**, *49*, 9743. [[CrossRef](#)]
29. Branca, C.; Di Blasi, C.; Galgano, A. Catalyst screening for the production of furfural from corncob pyrolysis. *Energy Fuels* **2012**, *26*, 1520. [[CrossRef](#)]
30. Di Blasi, C.; Branca, C.; Lombardi, V.; Ciappa, P.; Di Giacomo, C. Effects of particle size and density on the packed-bed pyrolysis of wood. *Energy Fuels* **2013**, *27*, 6781. [[CrossRef](#)]
31. Di Blasi, C.; Branca, C.; Sarnataro, F.E.; Gallo, A. Thermal runaway in the pyrolysis of some lignocellulosic biomasses. *Energy Fuels* **2014**, *28*, 2684. [[CrossRef](#)]
32. Branca, C.; Di Blasi, C.; Horacek, H. Analysis of the combustion kinetics and the thermal behaviour of an intumescent system. *Ind. Eng. Chem. Res.* **2002**, *41*, 2104. [[CrossRef](#)]
33. Branca, C.; Di Blasi, C.; Casu, A.; Morone, V.; Costa, C. Reaction kinetics and morphological changes of a rigid polyurethane foam during combustion. *Thermochim. Acta* **2003**, *399*, 127. [[CrossRef](#)]
34. Branca, C.; Di Blasi, C. A multi-step mechanism for the devolatilization of biomass fast pyrolysis oils. *Ind. Eng. Chem. Res.* **2006**, *45*, 5891. [[CrossRef](#)]
35. Branca, C.; Iannace, A.; Di Blasi, C. Devolatilization and combustion kinetics of Quercus Cerris bark. *Energy Fuels* **2007**, *21*, 1078. [[CrossRef](#)]
36. Branca, C.; Di Blasi, C. A unified mechanism of the combustion reactions of lignocellulosic fuels. *Thermochim. Acta* **2013**, *565*, 58. [[CrossRef](#)]
37. Trubetskaya, A.; Grams, J.; Leahy, J.J.; Johnson, R.; Gallagher, P.; Monaghan, R.F.D.; Kwapinska, M. The effect of particle size, temperature and residence time on the yields and reactivity of olive stones from torrefaction. *Renew. Energy* **2020**, *160*, 998. [[CrossRef](#)]
38. Shoulaifar, T.K.; DeMartini, N.; Zevenhoven, M.; Verhoeff, F.; Kiel, J.; Hupa, M. Ash-forming matter in torrefied birch wood: Changes in chemical association. *Energy Fuels* **2013**, *27*, 5684. [[CrossRef](#)]
39. Kim, S.; Park, J.K. Characterization of thermal reaction by peak temperature and height of DTG curves. *Thermochim. Acta* **1995**, *264*, 137. [[CrossRef](#)]

Disclaimer/Publisher's Note: The statements, opinions and data contained in all publications are solely those of the individual author(s) and contributor(s) and not of MDPI and/or the editor(s). MDPI and/or the editor(s) disclaim responsibility for any injury to people or property resulting from any ideas, methods, instructions or products referred to in the content.